

Control System of the Multi-rotor in Flight in the Presence of Strong Wind

LUCJAN SETLAK, RAFAŁ KOWALIK
Department of Avionics and Control Systems
Polish Air Force University
ul. Dywizjonu 303 nr 35, 08-521 Deblin
POLAND

l.setlak@law.mil.pl, r.kowalik@law.mil.pl, <http://www.law.mil.pl/index.php/pl/>

Abstract: - It is well known that the process of controlling a rotorcraft with a drive referred to as a rotor aircraft, in the event of adverse weather conditions, e.g. under the influence of strong wind, is the most difficult phase of the flight, requiring a lot of commitment and skill from the pilot/operator. This situation is confirmed by a relatively large number of aviation accidents that occur during the implementation of the process of controlling a multi-rotor in difficult weather conditions. In view of the above, it should be noted that the degree of difficulty of piloting an unmanned aircraft increases significantly when this operation is performed remotely by means of radio signals. As a consequence, the process of safely bringing an unmanned aircraft to the ground is extremely difficult even for an experienced operator who receives limited information about the flight condition of a multi-rotor. In view of the above, it is necessary to implement on-board control systems that enable automatic implementation of the flight stabilization process, e.g. during a storm. The key goal of this work is to design a multi-rotor control system based on the proposed algorithms for controlling unmanned aerial vehicles during high-wind flight, supported by a mathematical apparatus and selected simulation tests in the Matlab/Simulink environment. Based on the above, in the final part of this work, practical conclusions were formulated, reflecting the desirability of the tests carried out and confirmation of the results obtained.

Key-Words: - Control system, multi-rotor, mathematical analysis, influence of strong wind

1 Introduction

1.1 Unmanned aerial vehicles control system

The processes of piloting a multi-rotor in difficult environmental conditions are a small part of the entire flight that occurs just before its completion. During this short time, the pilot changes the airplane configuration and the power unit operating conditions to maintain certain flight parameters at a safe level. These activities also require the continuous tracking of a significant number of on-board instruments in correlation with information obtained from ground-based navigational aids and received visual channels. The approach and landing process requires a lot of commitment and high qualifications from the pilot [1], [2].

In addition, control in harsh atmospheric conditions, as the middle phase of the flight, is often performed after hours of flight in high-traffic airspace, this requires a lot of concentration from the operator, and can cause excessive fatigue and affect safety.

In order to relieve the operator, modern unmanned aircraft are equipped with automatic assistance systems, which also include automatic flight control systems with the possibility of automatic landing and maintaining flight stability.

Currently, automatic control systems have found wide application in both civil and military aviation.

They constitute the basic components of the on-board equipment of many manned aircraft, including General purpose aircraft GE (*General Aviation*), i.e. disposable, sanitary, etc., and so-called local communication (*Commuter*) or are also an indispensable element of unmanned systems. Their level of sophistication, quantity, quality and complexity largely depend on the type and category of aircraft, in particular the required level of safety, the amount of space available on board and the cost of production [3], [4].

In addition, it should be noted that automatic control systems were introduced to aviation primarily to relieve the pilot from monotonous performance of onerous activities related to manual piloting of aircraft, also enabling a significant increase in control precision and reducing the impact of human factor. In addition, in the case of unmanned aerial vehicles, they made it possible to fly long distances beyond the operator's range of vision when manual control is difficult or impossible [5], [6].

Their implementation on the aircraft causes that the actions performed by the pilot are limited to the

selection of the appropriate mode of operation of the system and the introduction of the desired parameters of its operation. The pilot's activity is limited to the function of the operator, managing the automatic operation of a technically complex machine, implementing the flight control process.

Growing with the development of technology, the trend in the field of advanced materials, electronics, sensors and batteries has caused that the dimensions and key technical parameters of micro unmanned aircraft have changed, among others, their size is in the range of 0.1 - 0.5 [m] in length and 0.1 - 5 [kg] in weight. Therefore, the class of unmanned vehicles with four rotors (*Quadrotor*) is becoming more and more popular, for which a lot of effort was put into developing new methods of their control and control system [7], [8].

An example of this type of object is HMX-4, which is a kind of 4-arm rotor weighing about 0.7 [kg] and length 76 [cm] between the ends of the rotor, whose flight time is about 3 minutes. It should be noted that due to the weight reduction of this type of unmanned aerial vehicle, both GPS (*Global Positioning System*) and other accelerometers cannot be added. Therefore, data on the location and speed of the object can be obtained through thermal imaging cameras [9], [10].

In order to obtain a feedback, it has an early MEMS (*Micro-Electro-Mechanical Systems*) system for pilot-assistant, designed to create small integrated devices or systems that combine mechanical and electrical components. In addition, the feedback linearization controller controls the height and angle of deviation. Due to the drift of the quadrotor in the x - y plane under the control of this controller, the reverse controller is needed to control the position.

Another commonly studied research field uses a proportional-integral-differentiating built-in PID controller (*Proportional - Integral - Derivative*), used to jointly control location and position, where *AscTec Hummingbird* is a typical model of this type of quadrotor [11], [12], [13].

This model is equipped with a frame made of wood or carbon fiber, making it durable and lightweight weighing about 0.5 [kg], it has its own sensors for obtaining states, and the controller used regulates the pressure in the installation based on the difference between the set and measured values. The next used PID control system is the STARMAC test table. The quadrotor object has a mass of about 1.1-1.6 [kg] and can carry an additional payload of about 2.5 [kg]. One of the path tracking models available outside is called the *X4-flyer* [14], [15].

The controller was developed in order to limit the vehicle orientation and keep it at a very low level,

while the created dynamic model was obtained by the *Euler-Langrage* method. For the purposes of performing simulation tests of this work, the PID controller was used to control an unmanned aerial vehicle in hover or track its flight path.

2 Dynamic analysis and quadrotor control model

The rotors are designed in such a way that it is possible to transfer the only force to the upper part of the quadrotor. It should be noted that the rotational speeds of the rotors also introduce torques. In turn, the forces and moments generated depend on the rotational speed of the rotor.

The main challenge is controlling the appropriate speeds of four rotors to ensure stable flight along the desired flight path of the vehicle [16], [17].

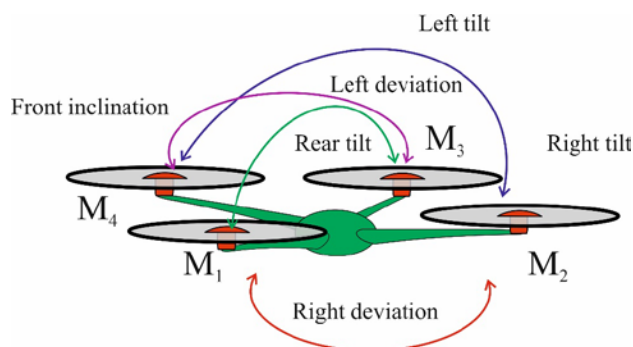


Fig. 1 A simplified illustration of rotor movement and quadrotor rotor control

The above figure (Fig. 1) shows a simplified way in which the rotors control the movement of the quadrotor rotor. It should be noted that the rotors 1 and 3 rotate counterclockwise and produce a clockwise torque. In contrast, the rotors 2 and 4 rotate clockwise and produce anti-clockwise torque. All 4 rotors generate upward force perpendicular to the plane of rotation. For the left digit in the figure above, the rotational speeds of rotors 2 and 4 are greater than the rotational speeds of rotors 1 and 3. Therefore, the effective torque will be generated in the counterclockwise direction, as a result of which the quadrotor will deflect in the counterclockwise direction [18], [19].

According to the right digit in the figure above, four rotors have the same rotational speed. The anti-clockwise momentum will balance the clockwise momentum, with the quadrotor being reversed when the sum of the lifting forces is greater than the force associated with gravity.

2.1 Dynamic model

To develop a dynamic quadrotor model, the body frame was positioned so that it was on the quadrotor

structure. As illustrated in the figure below (Fig. 2), the beginning of the body frame is centered at the 0 point of the quadrotor. One of his arms is selected as the X axis and the other as the Y axis.

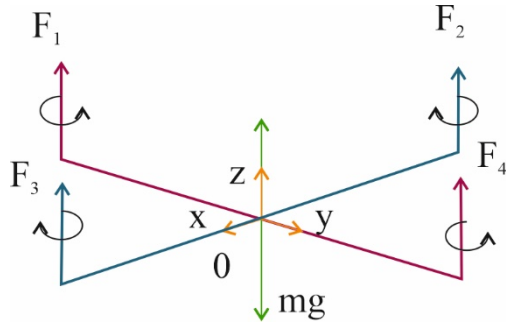


Fig. 2 Coordinate systems and forces/moments acting on the quadrotor frame

In the next figure (Fig. 3), the global frame is marked with the letter W and marked with the letters X_w, Y_w, Z_w , and the body frame is marked with the symbol B . The red lines of the chains are connected in a simple quadrotor scheme, and each line means quadrotor rotors.

The body frame is fixed at point 0, this point is the center of mass of the quadrotor rotor. The direction indicated from point 0 to rotor No. 1 is defined as the positive direction X_B , while the forward direction to rotor No. 3 is the negative direction X_B .

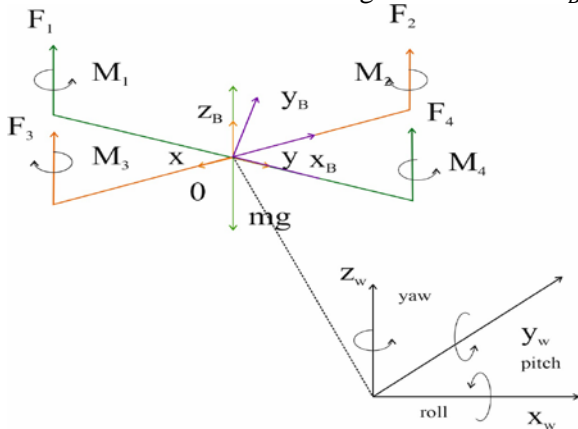


Fig. 3 Graph showing the deflection angles, tilt and inclination of the quadrotor

Similarly, the direction from point 0 to rotor No. 2 is defined as the positive direction Y_B , and the direction to rotor No. 4 is the negative direction Y_B . The Z_B direction is the direction from point 0 to the opposite direction of gravity.

In addition, in the figure above, rotation around Z_w by the angle of deviation ψ , rotation around the intermediate point X by the angle of tilt Φ , the rotor i rotates around the axis Y_B by the angle of inclination θ .

The rotation of the coordinate transformation matrix from B to W is (1) [20], [21]:

$$R = \begin{bmatrix} \cos\psi\cos\theta - \sin\psi\sin\theta & \cos\Phi\sin\psi & \cos\psi\sin\theta + \cos\theta\sin\Phi\sin\psi \\ \cos\theta\sin\psi + \cos\psi\sin\theta & \cos\Phi\cos\psi & \sin\psi\sin\theta - \cos\psi\cos\theta\sin\Phi \\ -\cos\Phi\sin\theta & \sin\Phi & \cos\Phi\cos\theta \end{bmatrix} m\ddot{r} = \begin{bmatrix} 0 \\ 0 \\ -mg \end{bmatrix} + R \begin{bmatrix} 0 \\ 0 \\ \sum F_i \end{bmatrix} \quad (1)$$

If r - means the vector of the position of the center of mass in the world frame, then the acceleration of the center of mass is determined by equation (2):

$$m\ddot{r} = \begin{bmatrix} 0 \\ 0 \\ -mg \end{bmatrix} + R \begin{bmatrix} 0 \\ 0 \\ \sum F_i \end{bmatrix} \quad (2)$$

where: p, q and r - determine the components of the angular speed of the robot in the body frame.

The relationship between these values and the derivatives of the deflection, tilt and inclination angle are expressed according to the following equation (3):

$$\begin{bmatrix} \dot{p} \\ \dot{q} \\ \dot{r} \end{bmatrix} = \begin{bmatrix} \cos\theta & 0 & -\cos\Phi\sin\theta \\ 0 & 1 & \sin\Phi \\ \sin\theta & 0 & \cos\Phi\cos\theta \end{bmatrix} \begin{bmatrix} \dot{\Phi} \\ \dot{\theta} \\ \dot{\psi} \end{bmatrix} \quad (3)$$

Each rotor i produces a moment M_i that is perpendicular to the plane of rotation. Impellers 1 and 3 generate moments in the direction $-Z_B$. The torques of impellers 2 and 4 are generated in the opposite direction: Z_B . The torque generated on the quadrotor is inverse to the direction of rotation of the blades, so M_1 and M_3 operate in the Z_B direction, while M_2 and M_4 operate in the opposite direction.

The distance from the axis of rotation of the rotors to the center of the rotor is marked with the letter L . By comparing the individual components of the quadrotor, the moment of inertia I is related to the center of gravity along the axis $X_B - Y_B - Z_B$.

Angular acceleration is obtained using Euler's equations, as shown below (4):

$$I = \begin{bmatrix} \dot{p} \\ \dot{q} \\ \dot{r} \end{bmatrix} = \begin{bmatrix} L(F_2 - F_4) \\ L(F_3 - F_1) \\ M_1 - M_2 + M_3 - M_4 \end{bmatrix} - \begin{bmatrix} p \\ q \\ r \end{bmatrix} \times I \begin{bmatrix} p \\ q \\ r \end{bmatrix} \quad (4)$$

2.2 Control model

2.2.1 Position control

This work presents the PID controller for controlling a quadrotor type object. The controller adjusts the process control inputs to minimize the error, which is the value of the difference between the measured process variable and the desired

setpoint, where the angle of tilt and inclination are located at the input.

By using the step back approach method, two types of position control methods can be obtained. One of them is the UAV (*Aerial Unmanned Vehicle*) hover regulator, whose key task is to control the operation of the rotor to maintain it in the desired position. The second is to control four rotors to track any trajectories in 3-D three-dimensional space.

2.1.2 Hinge adjuster

The quadrotor vehicle will hang at some point when the nominal propeller drive is equal to the force of gravity, so (5) [22], [23]:

$$F_{i,0} = \frac{mg}{4} \quad (5)$$

And rotational speed of the engine (6):

$$\omega_{i,0} = w_h = \sqrt{\frac{mg}{4k_F}} \quad (6)$$

where: $r_T(t)$ - is the position of the trajectory, $\psi_T(t)$ - are the angles of deviation, which are the path.

It should be remembered that the equation $\psi_T(t) = 0$ refers to the hinge regulator.

The position error is given by the next equation (7):

$$e_i = (r_{i,T} - r_i) \quad (7)$$

The set acceleration \ddot{r}_i^{des} can be calculated using the right PID controller (8):

$$\begin{aligned} (\ddot{r}_{i,T} - \ddot{r}_i^{des}) + k_{d,i}(\dot{r}_{i,T} - \dot{r}_i) \\ + k_{p,i}(r_{i,T} - r_i) \\ + k_{i,i} \int (r_{i,T} - r_i) = 0 \end{aligned} \quad (8)$$

Equation (9) is correct for hovering:

$$\dot{r}_{i,T} = \ddot{r}_{i,T} = 0 \quad (9)$$

The following formulas (10), (11) express the relationship between the desired accelerations and the tilt and inclination angles [24], [25]:

$$\begin{aligned} \ddot{r}_1^{des} &= g(\theta^{des} \cos\psi_T + \phi^{des} \sin\psi_T) \\ \ddot{r}_2^{des} &= g(\theta^{des} \sin\psi_T + \phi^{des} \cos\psi_T) \\ \ddot{r}_3^{des} &= \frac{8k_F\omega_h}{m} \Delta\omega_F \end{aligned} \quad (10)$$

$$\begin{aligned} \phi^{des} &= \frac{1}{g}(\ddot{r}_1^{des} \sin\psi_T - \ddot{r}_2^{des} \cos\psi_T) \\ \theta^{des} &= \frac{1}{g}(\ddot{r}_1^{des} \cos\psi_T - \ddot{r}_2^{des} \sin\psi_T) \\ \Delta\omega_F &= \frac{m}{8k_F\omega_h} \ddot{r}_3^{des} \end{aligned} \quad (11)$$

2.1.3 Altitude control

In the case of hovering, $\dot{\phi} \approx p, \theta \approx q, \psi \approx r$ $\dot{\Phi} \approx \dot{p}$, the proportional-derivative control law are used in the manner (12), (13) [26], [27]:

$$\begin{aligned} \Delta\omega_\phi &= k_{p,\phi}(\phi^{des} - \phi) + k_{p,\phi}(p^{des} - p) \\ \Delta\omega_\theta &= k_{p,\theta}(\theta^{des} - \theta) + k_{p,\theta}(q^{des} - q) \\ \Delta\omega_\psi &= k_{p,\psi}(\psi^{des} - \psi) + k_{p,\psi}(r^{des} - r) \end{aligned} \quad (12)$$

$$\begin{aligned} I_{xx}\dot{p} &= Lk_F(\omega_2^2 - \omega_4^2) - qr(I_{zz} - I_{yy}) \\ I_{yy}\dot{q} &= Lk_F(\omega_3^2 - \omega_1^2) - pr(I_{xx} - I_{zz}) \\ I_{zz}\dot{r} &= k_M(\omega_1^2 - \omega_2^2 - \omega_3^2 - \omega_4^2) \end{aligned} \quad (13)$$

The result of the above equation ω , is the result according to the following equation (14):

$$\begin{bmatrix} \omega_1^{des} \\ \omega_2^{des} \\ \omega_3^{des} \\ \omega_4^{des} \end{bmatrix} = \begin{bmatrix} 1 & 0 & -1 & 1 \\ 1 & 1 & 0 & -1 \\ 1 & 0 & 1 & 1 \\ 1 & -1 & 0 & -1 \end{bmatrix} \begin{bmatrix} \omega_h + \Delta\omega_F \\ \Delta\omega_\phi \\ \Delta\omega_\theta \\ \Delta\omega_\psi \end{bmatrix} \quad (14)$$

3 Dynamic model simulation

This chapter presents the numerical simulation results for dynamic and control model validation discussed earlier. The parameters used for the simulation are illustrated in the following table (Table 1).

Table 1. Parameters of the dynamic model

Kpx=1	Kpy=1	Kpz=1
Kdx=1	Kdy=1	Kdz=1
kF=6.11*10 ⁻⁸ N/(r/min ²)	KM=1.5*10 ⁻⁹ N/(r/min ²)	Km=20
M=1.08 kg	G=9.8 m/s ²	L=0.22 m

Based on the dynamic quadrotor model, the control model was developed in the Matlab/Simulink programming environment. In addition, for the purposes of simulation, the quadrotor flies from the initial position (0, 0, 0) to the final location (10, 10, 10) and hovers over this point (10, 10, 10), with the given distance units expressed in meters [m].

The figure below (Fig. 4) shows the actual path that the quadrotor follows.

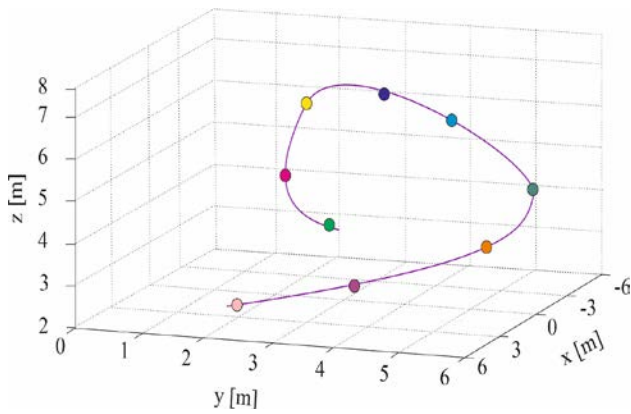


Fig. 4 The simulation result showing the trajectory of unmanned aerial vehicles

The next figures (Figs. 5-7) show graphs x , y , z of the quadrotor position as a function of time depending on the movement of this UAV from the initial to the desired (target) position.

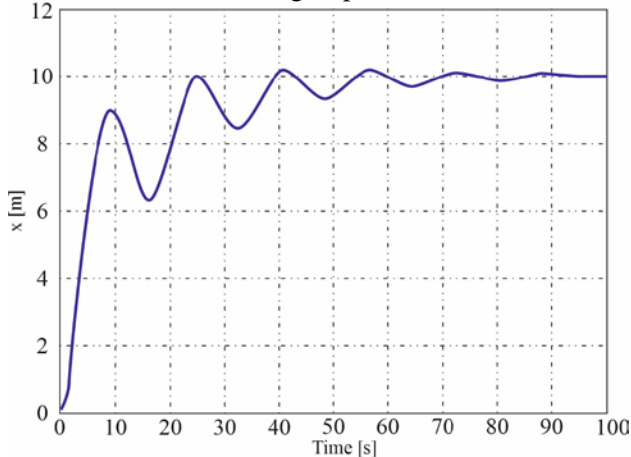


Fig. 5 The simulation result showing x position of the quadrotor relative to time

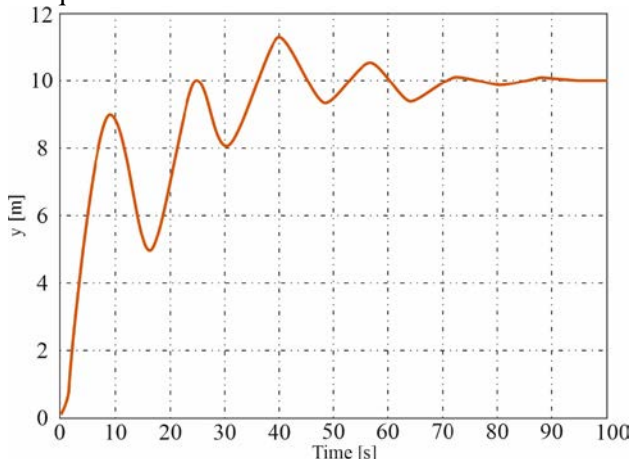


Fig. 6 The simulation result showing y position of the quadrotor relative to time

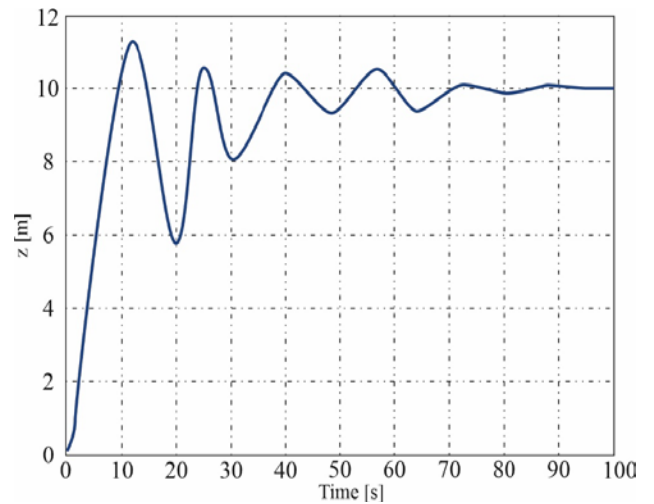


Fig. 7 The simulation result showing z position of the quadrotor as a function of time

In order to further verify the dynamic and control model in relation to tracking the desired trajectory (or rather, the location of the target), the quadrotor was put into motion in a circle at the center at point $(5, 0)$ and radius 5 [m].

The next figure (Fig. 8) shows a simulation of the result of the desired and real trajectory of the quadrotor following the circular trajectory.

The next figure (Fig. 9) shows the simulation result for the desired x and the actual x and the actual x for the circular path.

However, another figure (rys. 10) shows the simulation result that shows the desired y and real y for a circular path.

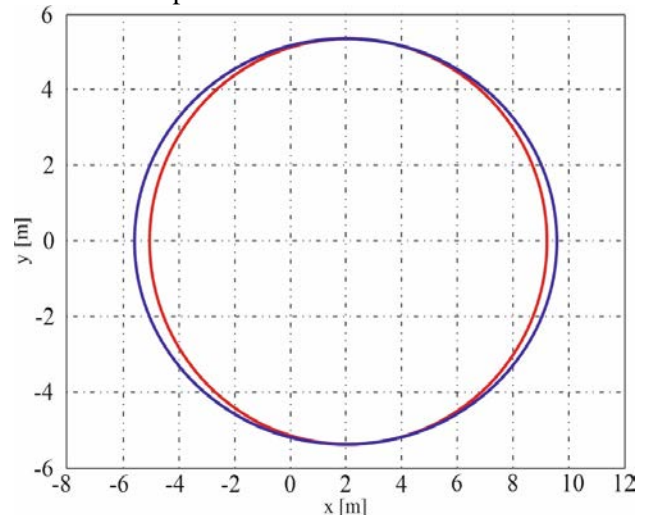


Fig. 8 Simulation result showing the desired (red) and real (blue) trajectory of a quadrotor following a circular trajectory

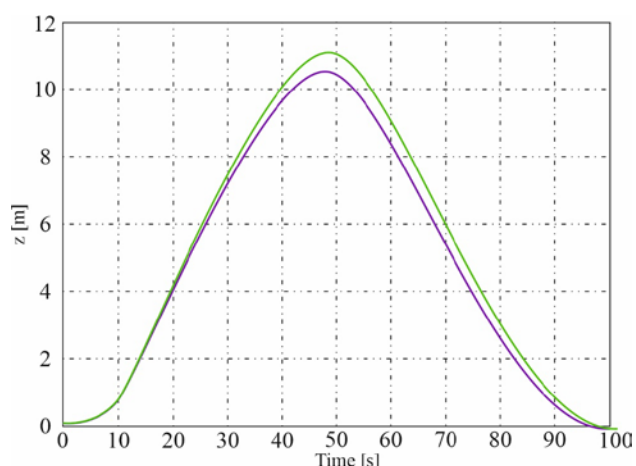


Fig. 9 Simulation result showing the desired x (red) and real x of a quadrotor on a circular trajectory

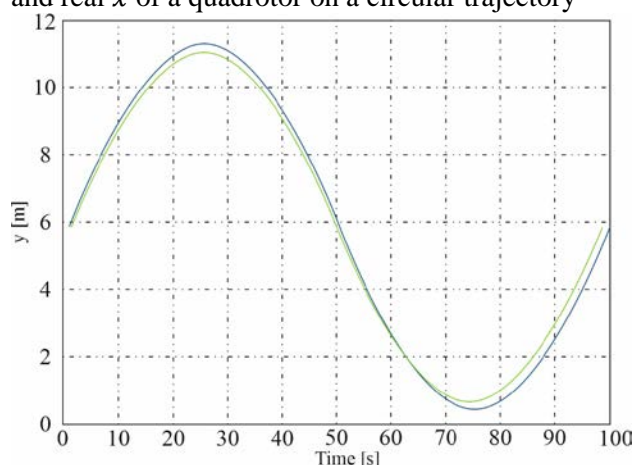


Fig. 10 Simulation result showing the desired y (red) and real y (blue) of a quadrotor on a circular trajectory

The control model was then verified showing that the quadrotor moves from rest position to the desired location and lands again.

The next figure (Fig. 11) presents a simulation of UAV object movement. The quadrotor started at point $(0, 0, 0)$ flew to point $(0, 0, 10)$, then it was rotated and moved to point $(10, 10, 10)$, and then landed at point $(10, 10, 0)$.

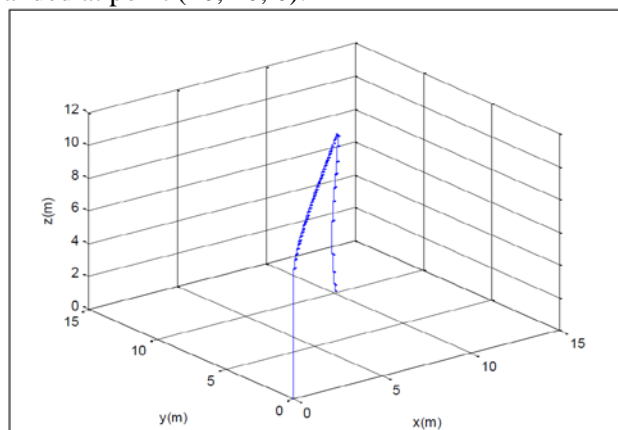


Fig. 11 Simulation of the result of quadrotor movement on the desired locations

The above numerical simulations showed that the quadrotor was able to navigate to any location of route points and follow any desired (given) trajectories.

4 Conclusions

The mathematical model of the four-rotor developed, after its linearization, was used to design the spatial orientation control system [28], [29], [30]. Positive results of simulation tests suggest that this system will also fulfill its task in real conditions.

Existing control algorithms can be expanded with superior systems that control altitude, position and flight trajectory, while striving for full autonomy of the aircraft. It should be noted that multi-rotor flying platforms are a relatively young and dynamically developing field.

Devices of this type find more and more applications, but they are still struggling with unsolved problems. Building a simple flying object of this type seems extremely simple, however, a project of this type obliges constructors and programmers to a serious challenge.

In addition, due to the nature of the platforms, it is necessary to use active thrust control to keep the robot in the air. Although simple PID controllers are enough to stabilize the flight, achieving control quality that allows the practical use of such platforms is still a challenge.

The first obstacle to achieving this is the incorrect design of the mechanical construction. Multi-rotors as flying apparatuses must have a very low unladen weight, while ensuring adequate rigidity and strength. At the same time, the key issue is the quality of orientation measurement, which is necessary in the process of platform stabilization [31], [32], [33].

As the rigidity of the supporting structure increases, the quality of regulation improves due to the smaller impact of structure deformations on enforcements and measurements. At the same time, however, the impact of disturbances generated by moving parts, especially drive units, increases in the quality of measurements.

This work mainly focuses on solving two problems, namely:

1. On obtaining a dynamic quadrotor model.
2. Possibilities of route planning and route planning optimization.

In the case of solving the first problem, the dynamics of the quadrotor were analyzed, and then a controller based on the PID method was developed.

In this part, the parameters were selected that were to make this simulation model almost identical to a real quadrotor. Then point-to-point navigation and trajectory experiments were carried out using a simulation model developed based on quadrotor dynamics.

The obtained results showed that this model proved to be useful in practical applications. Regarding the second problem, a trajectory was developed to fully cover a specific area.

The trajectory parameters were identified and the *Lanrage's* multiplier algorithm was used to obtain those parameters that minimized the total time needed to pass the entire quadrotor flight trajectory.

References:

- [1] K.P. Valavanis, G.J. Vachtsevanos, Handbook of Unmanned Aerial Vehicles, *Springer*: Dordrecht, The Netherlands, 2015.
- [2] M. Jafari, H. Xu, L.R.G. Carrillo, Brain Emotional Learning-Based Intelligent Controller for flocking of Multi-Agent Systems. In *Proceedings of the American Control Conference (ACC)*, Washington, DC, USA, 24-26 May 2017; pp. 1996-2001.
- [3] M. Jafari, On the Cooperative Control and Obstacle Avoidance of Multi-Vehicle Systems. *Master's Thesis, University of Nevada, Reno, NV, USA, 2015.*
- [4] A. Nourmohammadi, M. Jafari, T.O. Zander, A Survey on Unmanned Aerial Vehicle Remote Control Using Brain-Computer Interface, *IEEE Transactions on Human-Machine Systems*, Volume 48, Issue 4, 2018, pp. 337-348.
- [5] L. Setlak, R. Kowalik, Examination of the Unmanned Aerial Vehicle, ITM Web of Conferences 24, 01006, 2019.
- [6] R.A.S. Fernández, S. Dominguez, P. Campoy, L1 adaptive control for Wind gust rejection in quad-rotor UAV wind turbine inspection. In *Proceedings of the 2017 International Conference on Unmanned Aircraft Systems (ICUAS)*, Miami, FL, USA, 13-16 June 2017, pp. 1840-1849.
- [7] A. Cho, J. Kim, S. Lee, and C. Kee, Wind Estimation and Airspeed Calibration using a UAV with a Single-Antenna GPS Receiver and Pitot Tube, *IEEE Transactions on Aerospace and Electronic Systems*, Vol. 47, Issue 1, 2011, pp. 109-117.
- [8] A. Kroonenberg, T. Martin, M. Buschmann, J. Bange, and P. Vorsmann, Measuring the Wind Vector Using the Autonomous Mini Aerial Vehicle M2AV, *American Meteorological Society*, Vol. 25, 2008, pp. 1969-1982.
- [9] M. Allen, and V. Lin, Guidance and Control of an Autonomous Soaring UAV, NASA/TM-2007-214611, 2007.
- [10] H.S. Choi, S. Lee, J. Lee, E.T. Kim, and H. Shim, Aircraft Longitudinal Auto-landing Guidance Law Using Time Delay Control Scheme, *The Japan Society for Aeronautical and Space Sciences*, Vol. 53, 2010, pp. 207-214.
- [11] L. Setlak and R. Kowalik, MEMS Electro-mechanical Microsystem as a Support System for the Position Determining Process with the Use of the Inertial Navigation System INS and Kalman Filter, *WSEAS Transactions on Applied and Theoretical Mechanics*, Vol. 14, 2019, pp. 105-117.
- [12] L.R.G. Carrillo, A.E.D. López,; R. Lozano, C. Pégard, Quad Rotorcraft Control: Vision-Based Hovering and Navigation; *Springer*: Berlin, Germany, 2012.
- [13] S.L. Waslander, J.S. Jang, C.J. Tomlin, Multi-Agent X4-Flyer Testbed Control Design: Integral Sliding Mode vs. Reinforcement Learning, *IEEE Conference on Intelligent Robots and Systems*, 2009.
- [14] N. Guenard, T. Hamel, V. Moreau, and S.A. France, Dynamic Modeling and Intuitive Control Strategy for an X4-flyer, in *ICCA'05 International Conference on Control and Automation*, 2005, pp. 1-6.
- [15] M. Jafari, S. Sengupta, H.M. La, Adaptive Flocking Control of Multiple Unmanned Ground Vehicles by Using a UAV. In *Advances in Visual Computing: 11th International Symposium, ISVC 2015, Proceedings, Part II*, Las Vegas, NV, USA, 14-16, December 2015.
- [16] Y. Zhang, B. Xu, H. Li, Adaptive Neural Control of a Quadrotor Helicopter with Extreme Learning Machine, In *Proceedings of ELM-2014; Springer*: Berlin, Germany, Vol. 2, 2015, pp. 125-134.
- [17] B. Xian, C. Diao, B. Zhao, Y. Zhang, Nonlinear robust output feedback tracking control of a quadrotor UAV using quaternion representation. *Nonlinear Dynamics*, Vol. 79, 2015, pp. 2735-2752.
- [18] G. Bebis, R. Boyle, B. Parvin, D. Koracin, I. Pavlidis, R. Feris, T. McGraw, M. Elendt, R. Kopper, E. Ragan, et al., Eds.; *Springer*: Cham, Switzerland, 2015; pp. 628-637.
- [19] M. Jafari, A.M. Shahri, S.B. Shouraki, Attitude control of a quadrotor using brain emotional

- learning based intelligent controller. In *Proceedings of the 2013 13th Iranian Conference on Fuzzy Systems (IFSC)*, Tehran, Iran, 27-29 August 2013; pp. 1-5.
- [20] S. Lee, J. Lee, and D.S. Lee, Lateral and Directional SCAS Controller Design Using Multidisciplinary Optimization Program, *Journal of the Korean Society for Aeronautical & Space Sciences*, Vol. 40, Issue 3, 2012, pp. 251-257.
- [21] D. N. Axford, On the Accuracy of Wind Measurements Using an Inertial Platform in an Aircraft, and an Example of a Measurement of the Vertical Mesostructure of the Atmosphere, *Journal of Applied Meteorology*, Vol. 7, 1968, Issue 4, pp. 645-666.
- [22] S. Yoon and Y. Kim, Constrained Adaptive Backstepping Controller Design for Aircraft Landing in Wind Disturbance and Actuator Stuck, *International Journal for Aeronautical and Space Sciences*, 13 (2012), pp. 74-89.
- [23] L. Setlak, R. Kowalik, S. Bodzon, The Study of Air Flows for an Electric Motor with a Nozzle for an Unmanned Flying Platform, *WSEAS Transactions on Fluid Mechanics*, Vol. 14, 2019, pp. 21-35.
- [24] L.J. Bjarke, and L.J. Ehernberger, An In-Flight Technique for Wind Measurement in Support of the Space Shuttle Program, NASA TM 4154, 1989, pp. 3-4.
- [25] C. Coza, C. Nicol, C. Macnab, A. Ramirez-Serrano, Adaptive fuzzy control for a quadrotor helicopter robust to wind buffeting, *Journal of Intelligent and Fuzzy Systems*, Vol. 22, Issue 5, 2011, pp. 267-283.
- [26] H. Bou-Ammar, H. Voos, W. Ertel, Controller design for quadrotor UAVs using reinforcement learning. In *Proceedings of the 2010 IEEE International Conference on Control Applications (CCA)*, Tokyo, Japan, 8-10 September 2010, pp. 2130-2135.
- [27] S. Islam, M. Faraz, R. Ashour, G. Cai, J. Dias, L. Seneviratne, Adaptive sliding mode control design for quadrotor unmanned aerial vehicle, In *Proceedings of the 2015 International Conference on Unmanned Aircraft Systems (ICUAS)*, Denver, CO, USA, 9-12 June 2015, pp. 34-39.
- [28] J.W. Langelaan, N. Alley, and J. Neidhoefer, Wind Field Estimation for Small Unmanned Aerial Vehicles, *AIAA Guidance, Navigation and Control Conference*, 2010.
- [29] L. Setlak, R. Kowalik, Stability Evaluation of the Flight Trajectory of Unmanned Aerial Vehicle in the Presence of Strong Wind, *WSEAS Transactions on Systems and Control*, ISSN/E-ISSN: 1991-8763/2224-2856, Volume 14, , Art. #6, pp. 43-50, 2019.
- [30] D. Noble, S. Bhandari, Neural network based nonlinear model reference adaptive controller for an unmanned aerial vehicle. In *Proceedings of the 2017 International Conference on Unmanned Aircraft Systems (ICUAS)*, Miami, FL, USA, 13-16 June 2017; pp. 94-103.
- [31] L. Setlak, R. Kowalik, Stability Evaluation of the Flight Trajectory of Unmanned Aerial Vehicle in the Presence of Strong Wind, *WSEAS Transactions on Systems and Control*, Vol. 14, 2019, pp. 51-56.
- [32] P.B. Sujit, Srikanth Saripalli, and Joao Borges Sousa, Unmanned aerial vehicle path following: A survey and analysis of algorithms for fixed-wing unmanned aerial vehicles, *IEEE Control Systems*, 34(1): 2014, pp. 42-59.
- [33] N. Michael, D. Melinger, Q. Lindsey, and V. Kumar, The GRASP Multiple Micro UAV Testbed, *Robotics & Automation Magazine*, IEEE, 2010, pp. 56-65.